IJME

Int. J. of Applied Mechanics and Engineering, 2024, vol.29, No.3, pp.32-46
DOI: 10.59441/ijame/190394

THERMAL DIFFUSION AND DIFFUSION THERMO EFFECTS ON AXI-SYMMETRIC BOUNDARY LAYER FLOW OF NANOFLUID DUE TO NON-LINEAR STRETCHING SHEET ALONG THE RADIAL DIRECTION IN PRESENCE OF MAGNETIC FIELD

Upender Reddy Ganga*
Department of Mathematics, Nizam College (A), Osmania University, INDIA
E-mail: yuviganga@gmail.com

Ch. Janaiah
Department of Mathematics, Government Degree College, Sherilingampally Telangana, INDIA

B. Shankar Goud
Department of Mathematics, JNTUH College of Engineering, Science & Technology, INDIA

This work presents the results of numerical research that was conducted on the flow of axisymmetric nanofluids through a nonlinearly stretched sheet in the radial direction while a magnetic field influence was present. This model of a nanofluid demonstrates the presence of both the Brownian motion and the thermophoretic nanoparticle diffusion effects simultaneously. When calculating the flow, both the Dufour effect and the Soret effect are taken into consideration. The conservation of energy, species, and momentum is represented by the equations for this process. The transformation of partial differential equations can be achieved by utilizing similarity conversions. These equations take into account all of the thermophysical characteristics. Therefore, a feasible solution may be found in the Runge-Kutta approach. Graphic representations of the profiles for velocity, temperature, and concentration, along with evaluations of a few other parameters, are shown When compared to some of the earlier studies, the R-K code's validity is shown to be beyond question. Brownian motion *Nb* and Dufour effect *Du* lead to an increase in the temperature gradient. The results provide some insight into how the nanofluid is used in various commercial endeavours.

Key words: thermal diffusion, nanofluid, axi-symmetric flow, non-linearly stretching sheet, Runge-Kutta method.

1. Introduction

The inability of certain heat transfer fluids to maintain the required cooling efficiency is a common issue. This is because their thermal conductivities are lower than those of their counterparts. Some of the common fluids that have poor conductivities. It is possible to improve the thermal performance of fluids by adding ultra-fine particles into them. Because of their unique characteristics, people believe that nanofluids can significantly enhance the conductivity of various heat transfer fluids. Their scientific and industrial applications include nuclear reactors and cooling electronic devices. In addition, these fluids can be utilized in treating cancer. The first individual to refer to them as nanofluids [1]. In order to study the thermal performance of various fluids, a scientific model was developed by Buongiorno [2]. It also accounts for the Brownian motion and thermophoresis. The flow of the MHD boundary layer in a nanofluid with convective boundary constraints across a nonlinear stretching sheet was studied by Alkahtani and Abel [3]. Elazem [4] investigated how the flow of MHD nanofluids affects mass and heat transport over a stretched surface using numerical data. A permeable stretching/shrinking sheet with heat radiation impact was studied by Yashkun *et al.* [5] for the MHD hybrid nanofluid flow. In addition, Patel *et al.* [6] studied the MHD flow characteristics through a

* To whom correspondence should be addressed

stretching and shrinking sheet under radiation exposure. Alotaibi *et al.* [7] focused on Casson's flow characteristics in a non-linear manner. They noted that these factors influence the fluids' suction, injection, and viscous dissipation. For their study, Ali [8] utilized a finite element method to analyze the Casson nano liquid's rotating motion.

Different experimental and theoretical approaches to the heat transfer in nanofluids. This topic has received a lot of attention because of its distinctive applicability in many sectors, including manufacturing and production. In addition to energy storage devices, nanofluids can also be utilized for various industrial processes, such as heat exhaust systems and nuclear waste storage. The diffusion-thermos effect is a subset of Dufour that occurs when a concentration gradient is increased. It is referred to as a diffusion-thermos process when the gradient in concentration helps to facilitate the transfer of heat, and it is referred to as a thermo-diffusion process when the gradient in temperature helps to facilitate the transfer of mass. Another component of the substance's circulation is temperature differential. Mass flow can occur in the Soret Effect when a temperature difference causes a change in the flow rate. This can be useful when the flow area between densities is different. After conducting studies on ultra-small and large-scale fluids, scientists discovered the effects. Rasool *et al.* [9] studied effects on the flow of a nanofluid known as the Darcy-Forchheimer nanofluid. Zhang *et al.* [10] investigated the flow of pair stress fluids in microchannels caused by electromagnetic fields and characterized quadratic convection. Usman et al [11] noted that the continuous flow of micropolar fluids with the help and the pair stress was affected by the Dufour and Soret effects. Doing so allowed them to make more accurate predictions. Ahmed *et al.* [12] noted that the stretched cylinder causes the Dufour and Soret traits to appear in third-grade fluids. In another study, Bejawada *et al.* [13] explored the finite elements of the Dufour effect on the movement of mass and heat in an MHD flow. Hayat *et al.* [14] studied the effects of the Dufour and Soret activities on the movement of THNF's position flow using a spreadsheet. In another study, Uwanta *et al.* [15] a hydromagnetic fluid that had crossed a vertical surface. Mandal et al [16] utilized the Soret-Dufour interactions to study the conductivity of a hydromagnetic mass transport flow and heat electrodynamics in an infinite vertical plate. An investigation of the impacts of Soret and Dufour on mixed convection over a vertical wavy surface in a porous material with changing characteristics is carried out by Srinivasacharya [17]. Kumar *et al.* [18] conducted research on the Soret impact, which is a phenomenon that occurs when a nanofluid flows past a vertical plate in a porous media while being subjected to heat radiation. Sisko fluid flow via a non-Darcian micro-channel was studied by Bhatti *et al.* [19].

Particles in a nanofluid are so small that they are measured in nanometers. These solutions include nanoparticles in a synthetic colloidal suspension inside a base fluid. Nanofluids often include nanoparticles composed of carbides and metals. Fluids such as ethylene glycol, water, and oil are often used as bases. The unique characteristics of nanofluids offer them great promise for a wide range of uses, including but not limited to heat exchange, fuel cells, pharmaceutical processing, grinding, nuclear reactor coolant, and defence. Later on Heat and mass transport study of radiative and chemical reactive impacts on MHD nanofluid across an infinite moving vertical plate by Arulmozhi *et al*. [20]. Axisymmetric stagnation-point nanofluid flow across a stretched surface was explored by Nawaz and Hayat [21]. Mustafa *et al.* [22] investigated analytical and numerical solutions for nanofluid axisymmetric flow owing to non-linear sheet stretching. Ali *et al.* [23] studied variable viscosity effects on unsteady MHD axisymmetric nanofluid flow on a stretched surface with thermo-diffusion. Faiz *et al.* [24] examined many slip outcomes on time-dependent axisymmetric movement of magnetized Carreau nanofluid and motile microorganisms. Mahabaleshwar *et al.* [25] examined MHD and radiation effects on axisymmetric non-Newtonian fluid flow across a porous shrinking/stretching surface.

The current study is focused on the effects of a steady flow of a viscous that's incompressible and has a Brownian motion. The study also involves the use of nanoparticles that have thermophoretic diffusion capabilities. The investigation was carried out following a previous study. A new reality emerged from the study's findings. As a result, the exact answers to the equations without any dimensions were. This technique is employed to numerically resolve the numerical issues associated with dimensionless equations. The results are shown in a graphical representation. It shows the various parameters effects on the profiles of concentration. After doing several comparisons with earlier published work by Mustafa *et al.* [22] it was determined that the current investigation's findings are in substantial accord with those findings.

2. Flow governing equations

The following assumptions are made:
The fluid exhibits both incompressibility and conductivity. We can also choose a type of coordinate system that is cylindrical. Consider the incompressible movement of nanofluids that is aligned with the plane in Fig.1. It is located at the midpoint of the vertical axes' half-space z region. The sheet is stretched in the plane it's in while its velocity changes in the radial direction. The nanoparticle's mass flux is zero at the wall, while the sheet's temperature remains constant. The ambient values of nanoparticles are presented. The stretching velocity of the sheet is constant at the surface. When considering the induced magnetic field, it is assumed that it is smaller than the applied one, but neglected.

Continuity equation:

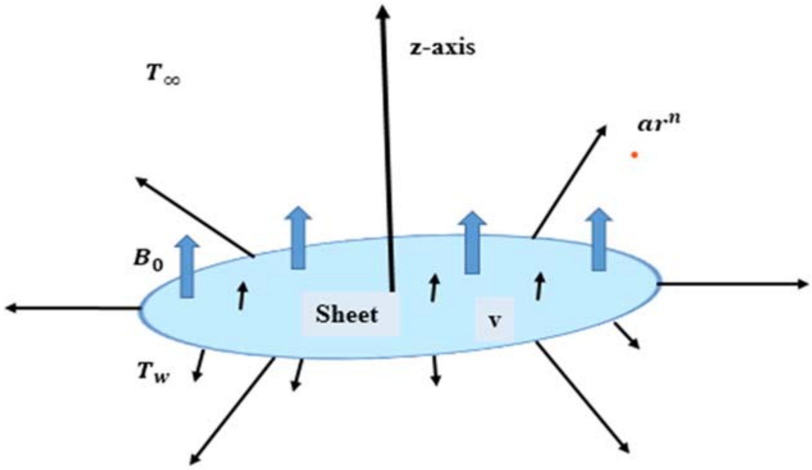

Fig.1. Flow geometry.

$$\left(\frac{\partial u}{\partial r}\right)+\left(\frac{r}{z}\right)+\left(\frac{\partial w}{\partial z}\right)=0\,. \tag{2.1}$$

Momentum equation:

$$u\left(\frac{\partial u}{\partial r}\right)+w\left(\frac{\partial u}{\partial z}\right)=\nu_f\left(\frac{\partial^2 u}{\partial z^2}\right)-\left(\frac{\sigma B_o^2}{\rho_f}\right)u\,. \tag{2.2}$$

Equation of thermal energy:

$$u\left(\frac{\partial T}{\partial r}\right)+w\left(\frac{\partial T}{\partial z}\right)=\alpha\left(\frac{\partial^2 T}{\partial z^2}\right)+\tau\left\{D_B\left[\frac{\partial C}{\partial z}\frac{\partial T}{\partial z}\right]+\frac{D_T}{T_\infty}\left[\frac{\partial T}{\partial z}\right]^2\right\}+\frac{D_m K_T}{C_s C_p}\left(\frac{\partial^2 C}{\partial z^2}\right). \tag{2.3}$$

Equation of species concentration:

$$u\left(\frac{\partial C}{\partial r}\right)+w\left(\frac{\partial C}{\partial z}\right)=D_B\left(\frac{\partial^2 C}{\partial z^2}\right)+\frac{D_T}{T_\infty}\left(\frac{\partial^2 T}{\partial z^2}\right)+\frac{D_m K_T}{T_m}\left(\frac{\partial^2 T}{\partial z^2}\right). \tag{2.4}$$

These are the boundary conditions that apply to nano-fluid flows.

$$\left.\begin{aligned} &u=u_w(r)=ar^n, \quad v=0, \quad T=T_w, \quad D_B\left(\frac{\partial C}{\partial z}\right)+\frac{D_B}{T_\infty}\left(\frac{\partial T}{\partial z}\right)=0 \quad \text{at} \quad z=0, \\ &u\to 0, \quad v=0, \quad T\to T_\infty, \quad C\to C_\infty \quad \text{as} \quad z\to\infty. \end{aligned}\right\} \tag{2.5}$$

In order to solve the governing Eqs (2.2)-(2.4), below variables have been introduced.

$$\left.\begin{aligned} &u=ar^n f'(\eta), \quad w=-ar^{\left(\frac{n-1}{2}\right)}\left(\sqrt{\frac{\nu_f}{a}}\right)\left(\left(\frac{n+3}{2}\right)f(\eta)+\left(\frac{n-1}{2}\right)\eta f'(\eta)\right), \\ &\eta=z\left(\sqrt{\frac{a}{\nu_f}}\right)r^{\left(\frac{n-1}{2}\right)}, \quad \psi=zf(\eta)\left(\sqrt{a\nu_f}\right), \quad \theta=\frac{T-T_\infty}{T_w-T_\infty}, \quad \phi=\frac{C-C_\infty}{C_\infty}. \end{aligned}\right\} \tag{2.6}$$

Employing Eq.(2.6), the Eqs (2.1) to (2.4) are transformed into:

$$f'''+\left(\frac{n+3}{2}\right)ff''-nf'^2-Mf'=0, \tag{2.7}$$

$$\theta''+\left(\frac{n+3}{2}\right)\Pr f\theta'+\Pr Nb\theta'\phi'+\Pr Nt\theta'^2+\Pr Du\phi''=0, \tag{2.8}$$

$$Nb\phi''+\left(\frac{n+3}{2}\right)ScNbf\phi'+Nt\theta''+NbScSr\theta''=0 \tag{2.9}$$

and Eq.(2.5) becomes:

$$\left.\begin{aligned} &f=0, \quad f'=1, \quad \theta=1, \quad Nb\phi'+Nt\theta'=0 \quad \text{at} \quad \eta=0, \\ &f'\to 0, \quad \theta\to 0, \quad \phi\to 0 \quad \text{as} \quad \eta\to\infty. \end{aligned}\right\} \tag{2.10}$$

The physical parameters of the given flow are specified concerning the boundary conditions.

$$\left.\begin{aligned} &\Pr=\frac{\nu_f}{\alpha}, \quad Sc=\frac{\nu_f}{D_B}, \quad M=\frac{\sigma B_o^2}{\rho_f a}, \quad Sr=\frac{D_m K_T(T-T_\infty)}{T_m\nu_f C_\infty}, \quad Du=\frac{D_m K_T C_\infty}{C_s C_p \nu_f (T-T_\infty)}, \\ &Nb=\frac{(\rho C)_p D_B C_\infty}{\nu_f(\rho C)_f}, \quad Nt=\frac{(\rho C)_p D_T(T_w-T_\infty)}{\nu_f T_\infty(\rho C)_f}. \end{aligned}\right\} \tag{2.11}$$

The physical interest, local Nusselt number, and skin friction coefficient parameters are presented in terms of their respective values.

$$Cf = \frac{\mu}{\rho_f u_w^2}\left(\frac{\partial u}{\partial z}\right)_{z=0} \Rightarrow \mathrm{Re}_r^{\frac{1}{2}}\, Cf = f''(0), \tag{2.12}$$

$$Nu_x = \frac{-r}{(T_w - T_\infty)}\left(\frac{\partial T}{\partial z}\right)_{z=0} \quad \text{where} \quad \Rightarrow \mathrm{Re}_r^{-\frac{1}{2}}\, Nu_x = -\theta'(0), \tag{2.13}$$

where $\mathrm{Re}_r = \dfrac{u_w r}{\nu_f}$ be the local Reynolds number.

3. Numerical solutions by shooting technique

The present investigation does not seem to have a definitive answer. The use of numerical processes is an essential component in the resolution of complicated problems in a wide variety of domains, including engineering, mathematics, and physics. The shooting and Runge-Kutta procedures are the two approaches that are applied the most often to BVPs. The following is a method to numerically solve the following regular differential equations with their corresponding boundary and initial conditions. For the first domain, the value of $[0,\infty)$ has been substituted with a bounded one. The first and second-order ODEs of Eqs (2.7) - (2.9) are prone to forming a highly nonlinear coupled boundary value problem. To minimize the number of initial problems encountered by the first-order unknowns, the conjecture for this problem has been reduced to seven.

$$f = y_1, \quad f' = y_2, \quad f'' = y_3, \quad \theta = y_4, \quad \theta' = y_5, \quad \phi = y_6, \quad \phi' = y_7. \tag{2.14}$$

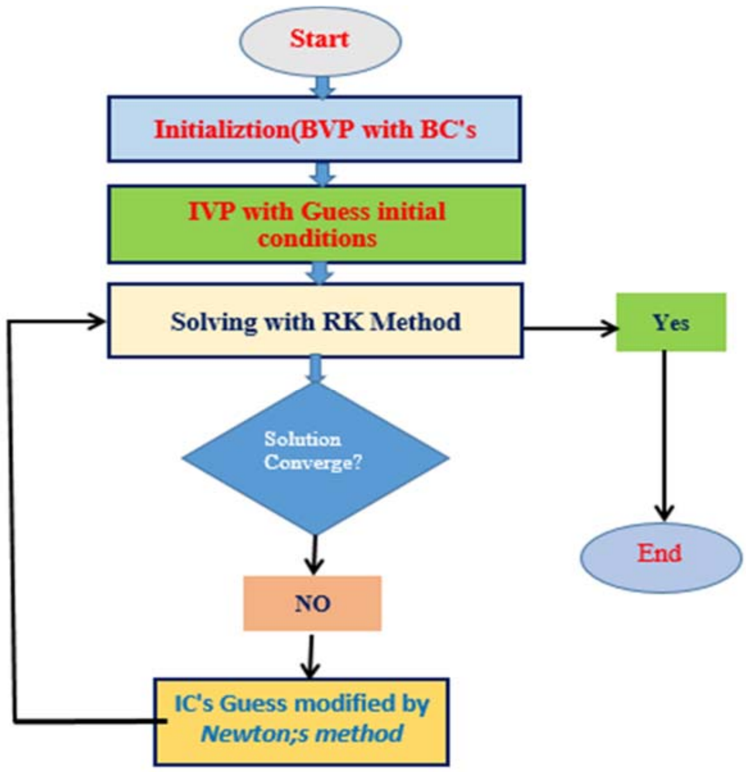

Fig.2. Flow chart of the problem solution.

The goal of this paper is to develop a numerical technique that is in line with the fourth-order shooting method. We use the MAPLE software to solve the problem. To perform this procedure, we need seven initial conditions. The numerical method is used to solve the problem by guessing the three initial conditions. The step size for the simulation is 0.001. If a solution does not satisfy the condition shown in Fig.2, the operation will repeat itself. Following is a flowchart of the problem, as well as the method for the RKF scheme, which may be found below.

4. Results and discussion

A non-linear PDE's Eqs (2.1)-(2.3) is converted to ODE's Eqs (2.7)-(2.9) using the stream functions, and similarity transformations, and numerically it is solved. The physical parameters of different velocity, concentration profiles, temperature profiles, and Brownian motion parameters are shown in Fig.3 through Fig.14. The profiles of different regions are shown in Figs 3, 4, and 5 respectively. The Power-law index values of these are shown in $n = 0.5, 1.0, 2.0$ and 3.0. On the other hand, n's slight influence on the nanoparticle concentration near the surface is notable. This is because, unlike in the case of the surface change, the nanoparticle concentration decreases in n. The nano-mass transfer rate and surface cooling rate increase with n values.

Table 1. The numerical values used to calculate the skin's friction coefficient.

n	M	Pr	Nt	Nb	Sr	Du	Sc	Cf
0.5	0.1	0.71	0.1	0.1	0.5	0.5	0.22	3.286781093784610
1.0								3.256781903761937
2.0								3.228718973460871
	0.5							3.246781093876908
	0.8							3.216589873109873
		1.00						3.246789198430369
		3.00						3.210785613736928
			0.2					3.346743160873155
			0.3					3.367676719736713
				0.5				3.33089818973311
				0.8				3.354418351045844
					1.0			3.330983418913618
					1.5			3.356786719819389
						1.0		3.340947389163191
						1.5		3.361435823562725
							0.30	3.240981609893394
							0.60	3.226671906387138

The relationship between the concentration and temperature profiles of a given region is explained by the Brownian motion parameter in Fig.6 and Fig.7. The increase in the temperature profiles, while the opposite occurs in the case of the concentration profiles. The temperature and thickness of nanoporous materials can increase due to their chaotic motion. This is because of the enhanced kinetic energy of the particles. Concentration also influences the motion of nanoparticles in different Brownian scenarios. The temperature and concentration profiles of a given region can be seen by comparing Fig.8 and Fig.9. The Thermophoresis parameter has a difference between these two measurements. The boundary layer thicknesses and temperature profiles of nanoparticles and their concentration profiles are considered to be moving functions of the Nt approximation. The temperature gradient effect known as the thermophoresis force can cause hotter molecules to move toward the low-temperature zone with greater kinetic energy. This can be used in various applications such as thermal precipitators and the transportation of polymeric molecules.

Table 2. Nusselt number values.

Pr	Nt	Nb	Du	n	Nu_x
0.71	0.1	0.3	0.5	0.5	1.854698190361934
1.00					1.796787193874022
3.00					1.750981908698649
	0.5				1.885694693468187
	0.8				1.917786859298763
		0.6			1.876678989379118
		0.8			1.909678719634838
			1.0		1.907878901297042
			1.5		1.934657221873483
				1.0	1.826776829040928
				2.0	1.806758902537803

The Prandtl number affects the thermal profiles of different materials. In this study, the thickness and temperature of thermal boundary layers are analyzed. The concentration profiles of different nanoparticles were measured for the Schmidt number. They can be seen in Fig.10. The Schmidt number is computed by taking into account the concentration and momentum boundary layers relative thickness. For instance, if Sc is small, the mass diffusion exceeds the momentum, resulting in a thicker concentration boundary layer. The velocity profiles can be explained by Fig.11. It is assumed that the affiliated thickness and fluid velocity contracted due to the magnetic parameter's enlargement. But the countermand trend can be observed in the temperature. The increase in the M value due to the Lorentz force's appreciation can be explained. This is because the force acts as a resistive force that prevents the fluid from moving.

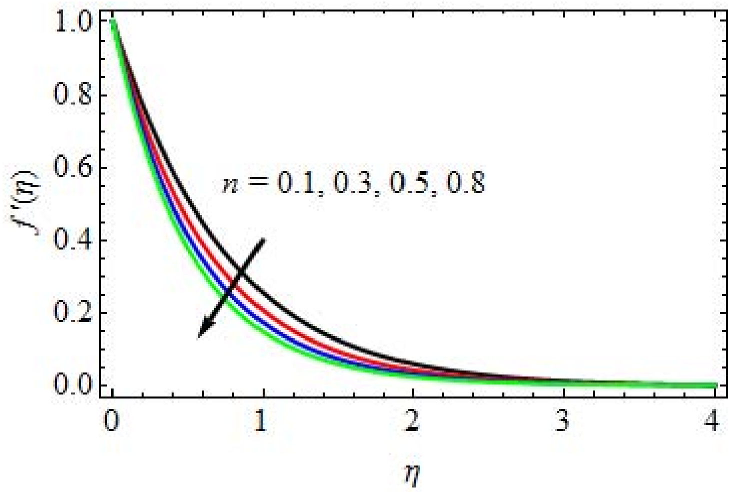

Fig.3. n Impact on velocity profiles.

The fluid's temperature profile increases with the Dufour number increasing seen in Fig.12. This phenomenon is believed to be caused by the release. The Soret number can increase the concentration profiles shown in Fig.13. This phenomenon is caused by the irreversible process, which can generate temperature gradients in a concentration field. It can also cause a spike in the flow system's concentration flux. Figure 14 presents the skin friction coefficient's numerical values for different engineering parameters' variations. Table 1 shows the different values of these parameters. The coefficient shows an increase or decrease in its values depending on the different parameters' variations. Table 2 and 3 shows the heat transfer coefficient and the varying effects of different parameter values on mass transfer coefficient.

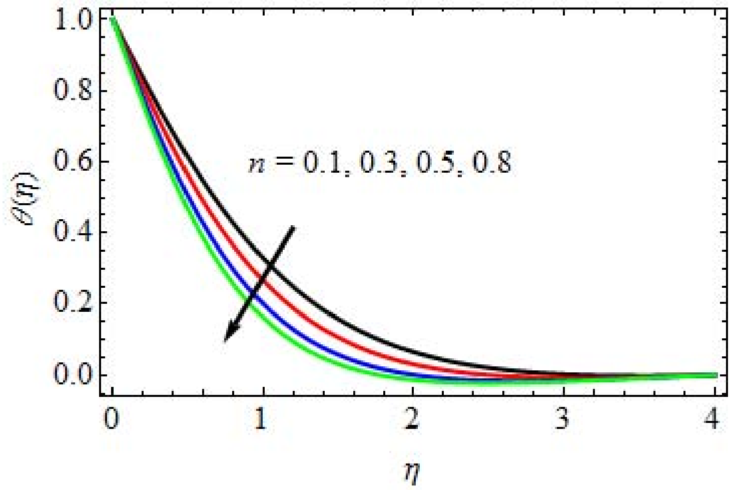

Fig.4. n impact on temperature profiles.

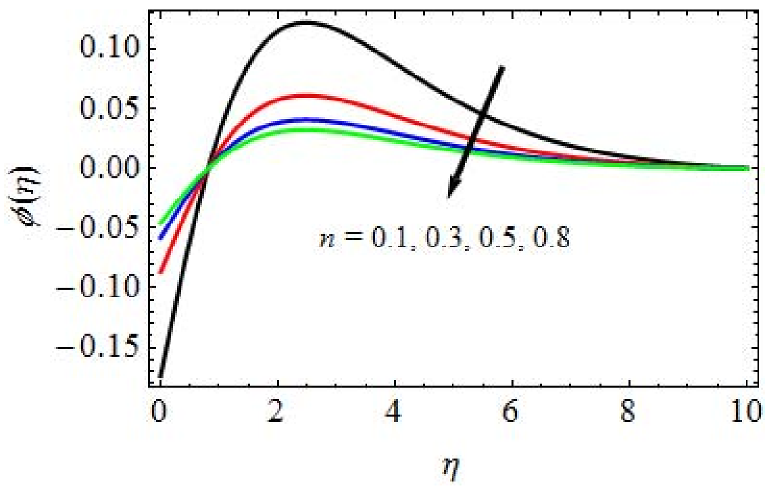

Fig.5. n impact on concentration profiles.

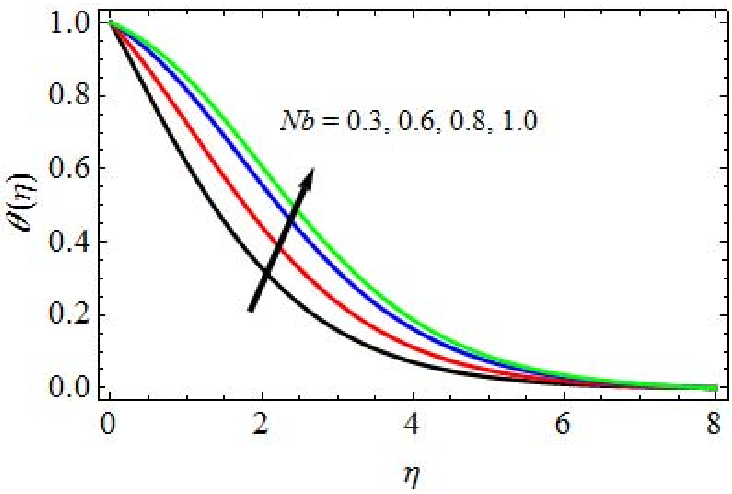

Fig.6. Nb Impact on temperature distribution.

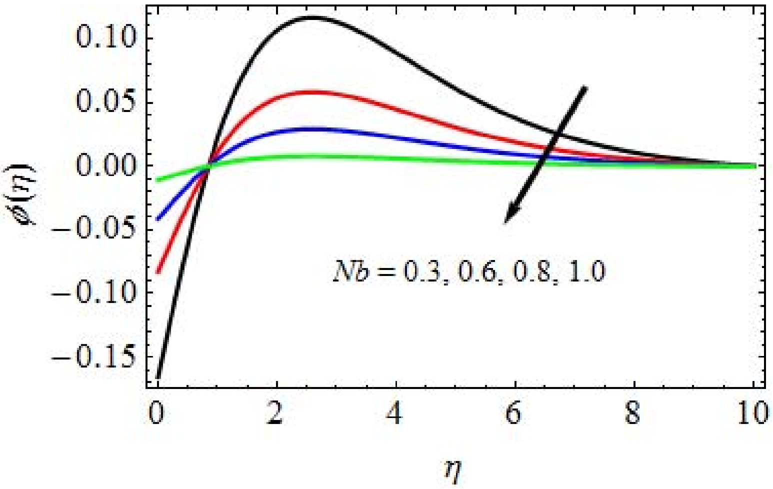

Fig.7. Nb Impact on concentration distribution.

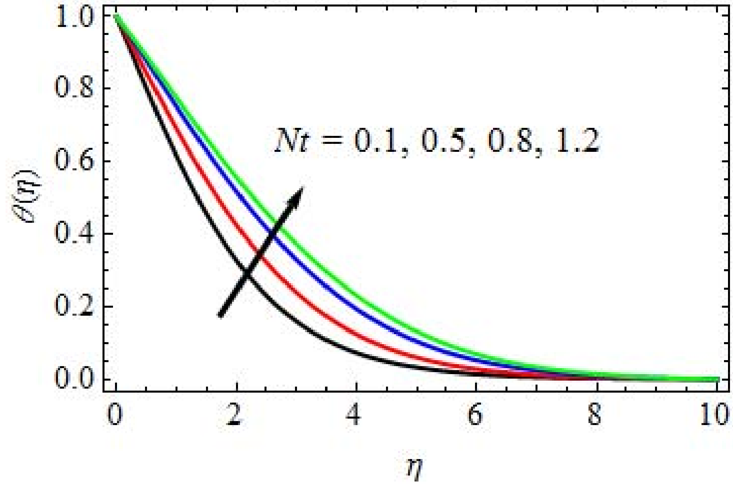

Fig.8. Nt impact on temperature distribution

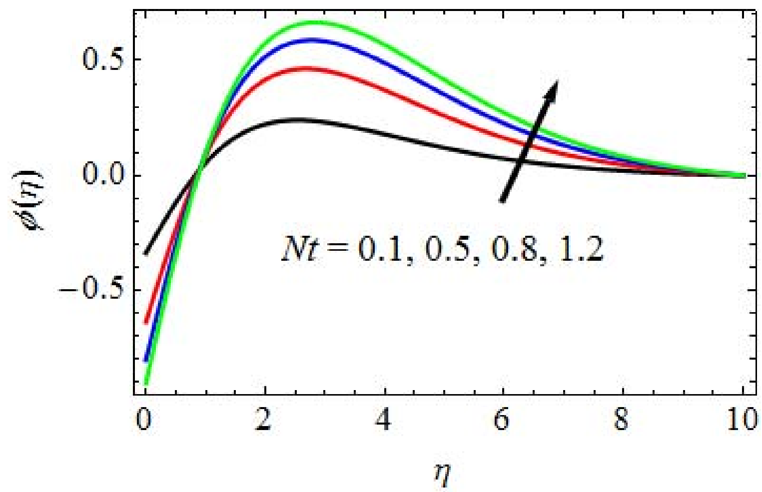

Fig.9. Nt impact on the concentration distribution

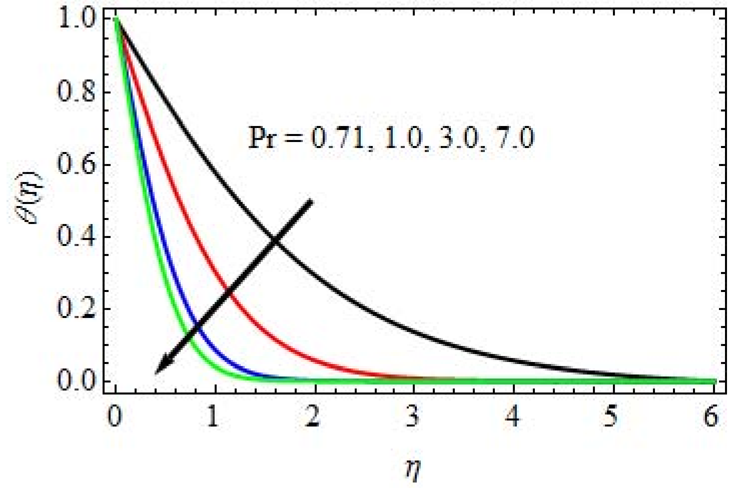

Fig.10. *Pr* Impact on temperature distribution.

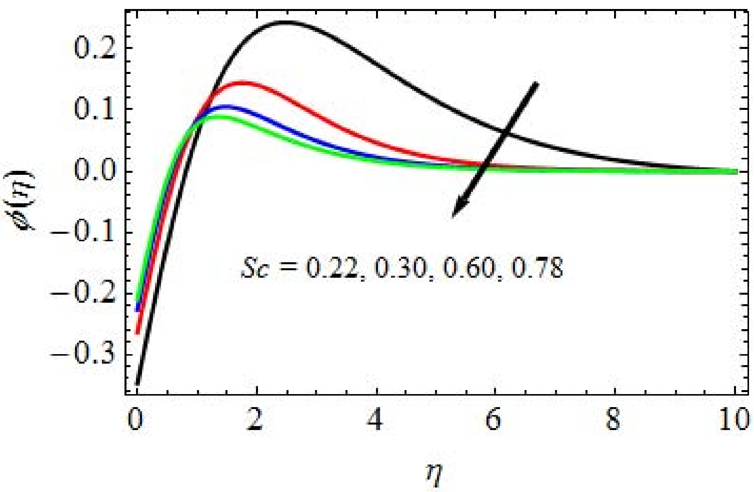

Fig.11. *Sc* Impact on concentration distribution.

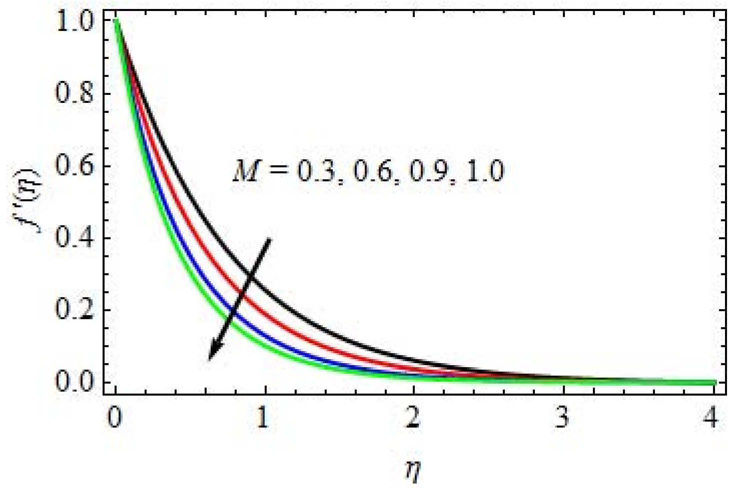

Fig.12. *M* impact on velocity distribution.

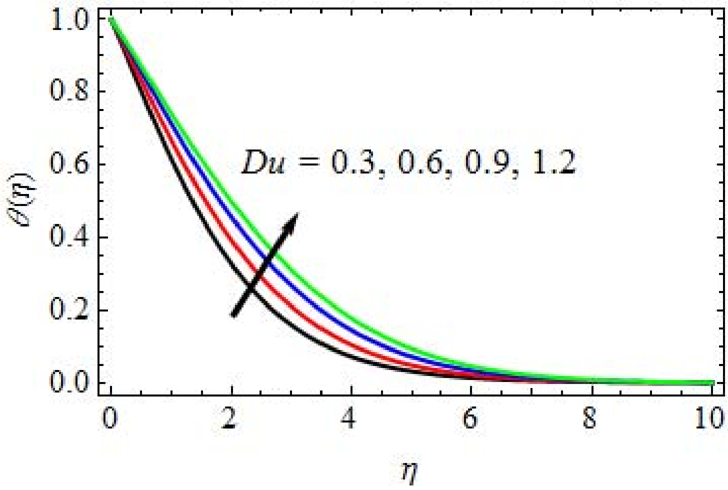

Fig.13. *Du* impact on temperature distribution.

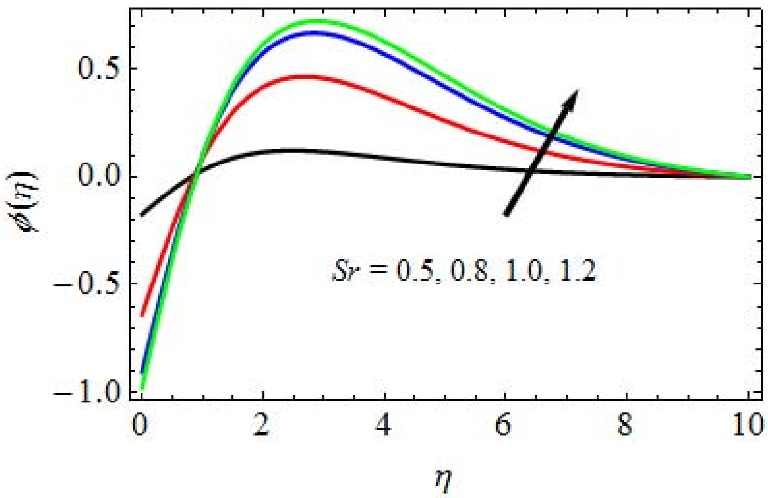

Fig.14. *Sr* impact on concentration distribution.

Table 3. Sherwood number values.

Sc	*Nt*	*Nb*	*Sr*	*n*	Sh_x
0.22	*0.1*	*0.3*	*0.5*	*0.5*	*2.176819387649381*
0.30					*2.106789027981349*
0.60					*2.057680920976928*
	0.5				*2.208907886738101*
	0.8				*2.232377509734172*
		0.6			*2.197768091897366*
		0.8			*2.220857138961399*
			1.0		*2.216780920398623*
			1.5		*2.236671378463461*
				1.0	*2.125678401039439*
				2.0	*2.105466176756480*

5. Program code validation

The acquired numerical results are verified by comparing the examination with Mustafa *et al.* [22] investigation in Tab.4. There is a strong basis for convergence among the two stated numerical continuations.

Table 4. Comparison of present reduced rate of heat transfer coefficient $-\theta'(0)$ for changed values of n, Nt, Sc and Pr.

n	Nt	Sc	Pr	Results of Mustafa *et al.* [22]	Present results
0.5	0.1	20.0	5.0	1.9112911	1.906741764376734
	0.5			1.2170065	1.207534718918389
	0.7			0.9815765	0.979617338734873
1.0	0.5	5.0	5.0	1.6914582	1.684657130457347
		10.0		1.4740787	1.468568310334739
		20.0		1.2861370	1.275665173746503
2.5	0.5	20.0	0.7	0.6619164	0.658670897885095
			5.0	1.4784288	1.469778970938450
			7.0	1.5758736	1.569670870263748

6. Conclusion

The goal of this research is to examine how thermos and thermal diffusion affect the boundary layer of two-dimensional nanostructures. The resulting flows are characterized by their incompressible, electrically conducting properties. They are also subjected to various motion effects. The analysis of this study involves converting non-linear equations into ordinary ones. The resulting approximations are then used in a shooting technique to perform a procedure known as similarity analysis. The physical flow factors are then studied and the conclusions are drawn.

- As the Power-law index and the impact of the magnetic field rise, the velocity flows diminish.
- The increase in the various motion factors, such as the Brownian motion (Nb), and Dufour effect (Du) leads to an enhancement in the thermal gradient. Also, higher values of the Power-law index and Prandtl number drop the temperature.
- The growth in the Thermophoresis and Soret number factors leads to a rise in the concentration profiles. Conversely, in the case of Brownian motion, Power-law index, and Schmidt number, the opposite outcome happens.

Applications

The findings of this study can help promote industrial production and quality nano-technology. It can also help develop a suitable combination of non-Newtonian fluids with other types of fluids for various applications in thermal sciences, chemical engineering, and biotechnology. Further studies on the flow in a confined annular or concentric cylinder can be performed.

Nomenclature

a – a constant parameter

B_o – uniform magnetic field

C – fluid concentration $\left[mol/m^3\right]$

Cf – skin-friction coefficient

C_f – specific heat capacity of base fluid $[J / kg\, K]$

C_p – specific heat at constant pressure $[J / kg\, K]$

C_s – concentration susceptibility

C_∞ – dimensional ambient volume fraction $\left[mol / m^3\right]$

D_B – thermophoresis diffusion coefficient $\left[m^2 / s\right]$

D_m – solutal diffusivity of the medium $\left[m^2 / s\right]$

D_T – Brownian diffusion coefficient $\left[m^2 / s\right]$

Du – Dufour number

f – dimensionless stream function

f' – fluid velocity $[m / s]$

K_T – thermal diffusion ratio

M – magnetic field parameter

n – power-law index parameter

Nb – Brownian motion parameter

Nt – thermophoresis parameter

Nu_x – Nusselt number

O – origin

$\Pr$ – Prandtl number

Re_r – Reynold's number

r, z – cylindrical coordinates $[m]$

Sc – Schmidt number

Sr – Soret number

T – fluid temperature $[K]$

T_m – fluid mean temperature

T_w – temperature at the surface $[K]$

T_∞ – the fluid's temperature distance from the stretched sheet $[K]$

u, w – velocity factors in r and z axes $[m / s]$

u_w – wall velocity along the r-coordinate $[m / s]$

greek symbols:

α – thermal diffusivity $\left[m^2 / s\right]$

η – dimensionless similarity variable

θ – dimensionless temperature $[K]$

κ – thermal conductivity of the fluid

μ – dynamic viscosity of the fluid

σ – electrical conductivity

ν_f – kinematic viscosity $\left[m^2/s\right]$

ρ_f – density $\left[kg/m^3\right]$

ρ_p – nano-fluid's density $\left[kg/m^3\right]$

φ – dimensional concentration $\left[mol/m^3\right]$

ψ – stream function

superscript:

$/$ – differentiation w.r.t η

subscripts:

f – fluid

w – condition on the sheet

∞ – ambient conditions

References

[1] Choi S.U.S. and Estman J.A. (1995): *Enhancing thermal conductivity of fluids with nanoparticles*.– ASME, FED231/MD vol.66, pp.99-105.

[2] Buongiorno J. (2006): *Convective transport in nanofluids*.– ASME, J. Heat Transf., vol.128, No.3, pp.240-250, https://doi.org/10.1115/1.2150834.

[3] Alkahtani B, Abel M.S. (2015): *MHD boundary layer flow over a nonlinear stretching sheet in a nanofluid with convective boundary conditio*n.– J. Comput. Theor. Nanosci., vol.12, No.12, pp.6020-6027, https://doi.org/10.1166/jctn.2015.4753.

[4] Abd Elazem N.Y. (2021): *Numerical results for influence the flow of MHD nanofluids on heat and mass transfer past a stretched surface*.– Nonlinear Eng.,vol.10, No.1, pp.28-38, https://doi.org/10.1515/nleng-2021-0003.

[5] Yashkun U, Zaimi K, Abu Bakar NA, Ishak A. and Pop I. (2021): *MHD hybrid nanofluid flow over a permeable stretching/shrinking sheet with thermal radiation effect*.– Int. J. Numer. Methods Heat Fluid Flow, vol.31, No.3, pp.1014-1031, https://doi.org/10.1108/HFF-02-2020-0083.

[6] Patel H.R., Mittal A.S. and Darji R.R. (2019): *MHD flow of micropolar nanofluid over a stretching shrinking sheet considering radiation*.– Int. Commun. Heat Mass Transf., vol.108, article 104322, https://doi.org/10.1016/j.icheatmasstransfer.2019.104322.

[7] Alotaibi H., Althubiti S., Eid M.R. and Mahny K.L. (2021): *Numerical treatment of MHD flow of Casson nanofluid via convectively heated non-linear extending surface with viscous dissipation and suction/injection effects*.– CMC-Computers, Materials & Continua, vol.66, No.1, pp.229-245, http://doi.org/10.32604/cmc.2020.012234.

[8] Ali B., Naqvi R.A., Haider A., Hussain D. and Hussain S. (2020): *Finite element study of MHD impacts on the rotating flow of Casson nanofluid with the double diffusion Cattaneo-Christov heat flux model*.– Mathematics, vol.8, No.9, p.1555, http://doi.org/10.3390/math8091555.

[9] Rasool G., Shafiq A. and Baleanu D. (2020): *Consequences of Soret-Dufour effects, thermal radiation and binary chemical reaction on Darcy-Forchheimer flow of nanofluids*.– Symmetry, vol.12, No.1, p.1421, http://doi.org/10.3390/sym12091421.

[10] Zhang L., Bhatti M.M., Michaelides E.E. and Ellahi R. (2024): *Characterizing quadratic convection and electromagnetically induced flow of couple stress fluids in microchannels*.– Qual. Theory Dyn. Syst., vol.23, No.1, p.35,. https://doi.org/10.1007/s12346-023-00883-z.

[11] Usman A.H., Shah Z., Humphries U.W., Kumam P. and Thounthong P. (2020): *Soret, Dufour and activation energy effects on double diffusive convective couple stress micropolar nanofluid flow in a Hall MHD generator system*.– AIP Adv., vol.10, No.7, article 075010, https://doi.org/10.1063/5.0014897.

[12] Ahmed B., Akbar F., Ghaffari A., Ullah Khan S., Khan M.I. and Dharmendar Reddy Y. (2022): *Soret and Dufour aspects of the third-grade fluid due to the stretching cylinder with the Keller box approach*.– Waves Random Complex Media, vol.32, https://doi.org/10.1080/17455030.2022.2085891.

[13] Bejawada S.G. and Yanala D.R. (2021): *Finite element Soret Dufour effects on an unsteady MHD heat and mass transfer flow past an accelerated inclined vertical plate*.– Heat Transfer, vol.50, No.8, pp.8553-8578, https://doi.org/10.1002/htj.22290.

[14] Hayat T., Khan M.I., Waqas M. and Ahmed A. (2017): *Stagnation point flow of hyperbolic tangent fluid with Soret and Dufour effects.*Results Phy., vol.7, pp.2711-2717, https://doi.org/10.1016/j.rinp.2017.07.014.

[15] Uwanta I.J., Asogwa K.K. and Ali U.A. (2012): *MHD fluid flow over a vertical plate with Dufour and Soret effects*. Int. J. Comput. Appl., vol.45, No.2, pp.8-16, http://doi.org/10.5120/6750-8998.

[16] Mandal B., Bhattacharyya K., Banerjee A., Kumar Verma A. and Kumar Gautam A. (2020): *MHD mixed convection on an inclined stretching plate in Darcy porous medium with Soret effect and variable surface conditions*.– Nonlinear Engineering, vol.9, No.1, pp.457-469, https://doi.org/10.1515/nleng-2020-0029.

[17] Srinivasacharya D., B. Mallikarjuna B. and Bhuvanavijaya. R. (2015): *Soret and Dufour effects on mixed convection along a vertical wavy surface in a porous medium with variable properties*.– Ain Shams Eng. J., vol.6, No.2, pp.553-564, http://doi.org/10.1016/j.asej.2014.11.007.

[18] Kumar A., Singh R., Seth G.S. and Tripathi R. (2018): *Soret effect on transient magnetohydrodynamic nanofluid flow past a vertical plate through a porous medium with second order chemical reaction and thermal radiation.*– Int. J. Heat Tech., vol.36, No.4, pp.1430-1437, https://doi.org/10.18280/ijht.360435.

[19] Bhatti M.M., Sarris I., Michaelides E.E. and Ellahi R. (2024): *Sisko fluid flow through a non-Darcian micro-channel: An analysis of quadratic convection and electro-magneto-hydrodynamics*.– Therm. Sci. Eng. Prog., vol.50, p.102531, https://doi.org/10.1016/j.tsep.2024.102531.

[20] Arulmozhi S., Sukkiramathi K., Santra S.S., Edwan R., Fernandez-Gamiz U. and Noeiaghdam S. (2022): *Heat and mass transfer analysis of radiative and chemical reactive effects on MHD nanofluid over an infinite moving vertical plate*.– Results in Engineering, vol.14, p.100394., https://doi.org/10.1016/j.rineng.2022.100394.

[21] Nawaz M. and Hayat T. (2014): *Axisymmetric stagnation-point flow of nanofluid over a stretching surface*.– Advances in Applied Mathematics and Mechanics, vol.6, No.2, pp.220-232., https://doi.org/10.4208/aamm.2013.m93.

[22] Mustafa M., Khan J.A., Hayat T. and Alsaedi A. (2015): *Analytical and numerical solutions for axisymmetric flow of nanofluid due to non-linearly stretching sheet*.– International Journal of Non-Linear Mechanics, vol.71, pp.22-29, https://doi.org/10.1016/j.ijnonlinmec.2015.01.005.

[23] Ali B., Naqvi R.A., Nie Y., Khan S.A., Sadiq M.T., Rehman A.U. and Abdal S. (2020): *Variable viscosity effects on unsteady MHD an axisymmetric nanofluid flow over a stretching surface with thermo-diffusion: Fem approach*.– Symmetry, vol.12, No.2, p.234, https://doi.org/10.3390/sym12020234.

[24] Faiz M., Habib D., Siddique I., Awrejcewicz J., Pawłowski W., Abdal S. and Salamat N. (2022): *Multiple slip effects on time dependent axisymmetric flow of magnetized Carreau nanofluid and motile microorganisms*.– Scientific Reports, vol.12, No.1, p.14259, https://doi.org/10.1038/s41598-022-18344-z.

[25] Mahabaleshwar U.S., Maranna T., Perez L.M. and Nayakar S.R. (2023): *An effect of magnetohydrodynamic and radiation on axisymmetric flow of non-Newtonian fluid past a porous shrinking/stretching surface*.– Journal of Magnetism and Magnetic Materials, vol.571, p.170538, https://doi.org/10.1016/j.jmmm.2023.170538.

Received: March 12, 2024
Revised: June 24, 2024